

Stick-slip statistics for two fractal surfaces: A model for earthquakes

Bikas K. Chakrabarti^{*,+} and Robin B. Stinchcombe^{*}

^{*}Theoretical Physics, Department of Physics, University of Oxford
1 Keble Road, Oxford, OX1 3NP, England.

⁺Saha Institute of Nuclear Physics
1/AF Bidhannagar, Calcutta 700064, India.

Abstract: Following the observations of the self-similarity in various length scales in the roughness of the fractured solid surfaces, we propose here a new model for the earthquake. We demonstrate rigorously that the contact area distribution between two fractal surfaces follows an unique power law. This is then utilised to show that the elastic energy releases for slips between two rough fractal surfaces indeed follow a Guttenberg-Richter like power law.

1. Introduction

The earth's solid outer crust, of about 20 kilometers in average thickness, rests on the tectonic shells. Due to the high temperature-pressure phase changes and the consequent powerful convective flow in the earth's mantle, at several hundreds of kilometers of depth, the tectonic shell, divided into a small number (about ten) of mobile plates, has relative velocities of the order of a few centimeters per year [1,2]. Over several tens of years, enormous elastic strains develop sometimes on the earth's crust when sticking (due to the solid-solid friction) to the moving tectonic plate. When slips occur between the crust and the tectonic plate, these stored elastic energies are released in 'bursts', causing the damages during the earthquakes. Because of the uniform motion of the tectonic plates, the elastic strain energy stored in a portion of the crust (block), moving with the plate relative to a 'stationary' neighbouring portion of the crust, can vary only due to the random strength of the solid-solid friction between the crust and the plate. The slip occurs when the accumulated stress exceeds the frictional force. As mentioned before, the observed distribution of the elastic energy release in various earthquakes seems to follow a power law. The number of earthquakes $N(m)$, having magnitude in the Richter scale greater than or equal to m , is phenomenologically observed to decrease with m exponentially. This gives the Guttenberg-Richter law [1]

$$\ln N(m) = \text{constant} - a m, \quad (1)$$

where a is a constant. It appears [1,2] that the amount of energy ϵ released in an earthquake of magnitude m is related to it exponentially:

$$\ln \epsilon = \text{constant} + b m, \quad (2)$$

where b is another constant. Combining therefore we get the power law giving the number of earthquakes $N(\epsilon)$ releasing energy greater than or equal to ϵ as

$$N(\epsilon) \sim \epsilon^{-\alpha}, \quad (3)$$

with $\alpha = a/b$. For most regions of the earth $a \simeq 1$. The estimates of b are more difficult, and vary between 1.0 and 1.5 [1,2]. Hence, the observed value of the exponent (power) α in (3) ranges between 0.7 and 1.0.

Several laboratory and computer simulation models have recently been proposed [3] to capture essentially the above power law in the earthquake energy release statistics. In a table-top laboratory simulation model of earthquakes, Burridge and Knopoff [4] took a chain of wooden blocks connected by identical springs to the neighbouring blocks. The entire chain was placed on a rigid horizontal table with a rough surface, and one of the end blocks was pulled very slowly and uniformly using a driving motor. The strains of the springs increase due to the creep motions of the blocks until one or a few of the blocks slip. The drops in the elastic energy of the chain during slips could be measured from the extensions or compressions of all the springs, and could be taken as the released energies in the earthquake. For some typical roughness of the surfaces (of the blocks and of the table), the distribution of these drops in the elastic energy due to slips indeed shows a power law behaviour with $\alpha \simeq 1$ in (3). A computer simulation version of this model by Carlson and Langer [5] considers harmonic springs connecting equal mass blocks which are also individually connected to a rigid frame (to simulate other neighbouring portions of the earth's crust not on the same tectonic plate) by harmonic springs. The entire system moves on a rough surface with nonlinear velocity dependent force (decreasing to zero for large relative velocities) in the direction opposite to the relative motion between the block and the surface. In the computer simulation of this model it is seen that the distribution

of the elastic energy release in such a system can indeed be given by a power law like (3), provided the nonlinearity of the friction force, responsible for the self-organisation, is carefully chosen [5]. The lattice automata model of Bak et al [6] and its modification appropriate to the Burridge-Knopoff model by Olami et al [6] represent the stress on each block by a height variable at each lattice site. The site topples (the block slips) if the height (or stress) at that site exceeds a preassigned threshold value, and the height becomes zero there and the neighbours share the stress by increasing their heights by one unit. With this dynamics for the system, if any of the neighbouring sites of the toppled one was already at the threshold height, the avalanche continues. The boundary sites are considered to be all absorbing. With random addition of heights at a constant rate (increasing stress at a constant rate due to tectonic motion), such a system reaches its self-organised critical point where the avalanche size distributions follow a natural power law corresponding to this self-tuned critical state. Bak et al [6] identify this self-organised critical state to be responsible for the Guttenberg-Richter type power law. All these models are successful in capturing the Guttenberg-Richter power law, and the real reason for the self-similarity inducing the power law is essentially the same in all these different models: emergence of the self-organised critical state for wide yet suitably chosen variety of nonlinear many-body coupled dynamics. In this sense all these models incorporate the well-established fact of the stick-slip frictional instabilities between the earth's crust and the tectonic plate. It is quite difficult to check at this stage any further details and predictions of these models.

While the motion of the tectonic plate is surely an observed fact, and this stick-slip process should be a major ingredient of any bonafide model of earthquake, another established fact regarding the fault geometries of the earth's crust is the fractal nature of the roughness of the surfaces of the earth's crust and the tectonic plate. This latter feature is missing in any of these models discussed above. In fact, the surfaces involved in the process are results of large scale fracture separating the crust from the moving tectonic plate. Any such crack surface is observed to be a self-similar fractal, having the self-affine scaling property $z(\lambda x, \lambda y) \sim \lambda^\zeta z(x, y)$ for the surface coordinate z in the direction perpendicular to the crack surface in the (x, y) plane [7]. Various fractographic investigations indicate a fairly robust universal behaviour for such surfaces and the roughness exponent ζ is observed to have a value around 0.80-0.85 (with a possible crossover to $\zeta \simeq 0.4$ for slow

propagation of the crack-tip) [8,3]. This widely observed scaling property of the fracture surfaces also suggests that the fault surfaces of the earth's crust or the tectonic plate should have similar fractal properties. In fact, some investigators of the earthquake dynamics have already pointed out that the fracture mechanics of the stressed crust of the earth forms self-similar fault patterns, with well-defined fractal dimensionalities near the contact areas with the major plates [9]. Although no realistic models have been developed incorporating this fact, these investigators [9] have often pointed out that such self-similarities of the fault surfaces could be responsible for the Guttenberg-Richter power law (3).

2. Model and RG calculations

In our model, the solid-solid contact surfaces of both the earth's crust and the tectonic plate are considered as average self-similar fractal surfaces. We then consider the distribution of contact areas, as one fractal surface slides over the other. We relate the total contact area between the two surfaces to be proportional to the elastic strain energy that can be grown during the sticking period, as the solid-solid friction force arises from the elastic strains at the contacts between the asperities [10]. We then consider this energy to be released as one surface slips over the other and sticks again to the next contact or overlap between the rough fractal surfaces. Considering that such slips occur at intervals proportional to the length corresponding to that area, we obtain a power law for the frequency distribution of the energy releases. This compares quite well with the Guttenberg-Richter law.

In order to proceed with the estimate of the number density $n(\epsilon)$ of earthquakes releasing energy ϵ in our model, we first find out the distribution $\rho(s)$ of the overlap or contact area s between two self-similar fractal surfaces. We then relate s with ϵ and the frequency of slips as a function of s , giving finally $n(\epsilon)$. To start with a simple problem of contact area distribution between two fractals, we first take two Cantor sets [11] to model the contact area variations of two (nonrandom and self-similar) surfaces as one surface slides over the other. Figure 1(a) depicts structure in such surfaces at a scale which corresponds to only the second generation of iterative construction of two displaced Cantor sets, shown in Fig. 1(b). It is obvious that with successive iterations, these surfaces will acquire self-similarity at every length scale, when the generation number goes to infinity. We intend to study the distribution of the total overlap s (shown by the shaded regions in

Fig. 1(b)) between the two Cantor sets, in the infinite generation limit. Let the sequence of generators G_l define our Cantor sets within the interval $[0,1]$: $G_0 = [0, 1]$, $G_1 \equiv RG_0 = [0, a] \cup [b, 1]$ (i.e., the union of the intervals $[0, a]$ and $[b, 1]$), \dots , $G_{l+1} = RG_l$, \dots . If we represent the mass density of the set G_l by $D_l(r)$, then $D_l(r) = 1$ if r is in any of the occupied intervals of G_l , and $D_l(r) = 0$ elsewhere. The required overlap magnitude between the sets at any generation l is then given by the convolution form $s_l(r) = \int dr' D_l(r') D_l(r - r')$. This form applies to symmetric fractals (with $D_l(r) = D_l(-r)$); in general the argument of the second D_l should be $D_l(r + r')$.

Some aspects of the convolution of two Cantor sets has previously been discussed [12] in connection with band-width and band number transitions in quasicrystal models. The generalisation given hereunder of the earlier employed recursive scaling method provides a very direct solution to the more complex problem we encounter here. One can express the overlap integral s_1 in the first generation by the projection of the shaded regions along the vertical diagonal in Fig. 2(a). That gives the form shown in Fig. 2(b). For $a = b \leq \frac{1}{3}$, the nonvanishing $s_1(r)$ regions do not overlap, and are symmetric on both sides with the slope of the middle curve being exactly double those on the sides. One can then easily check that the distribution $\rho_1(s)$ of overlap s at this generation is given by Fig. 2(c), with both c and d greater than unity, maintaining the normalisation of the probability ρ_1 with $cd = 5/3$. The successive generations of the density $\rho_l(s)$ may therefore be represented by Fig. 3, where

$$\rho_{l+1}(s) = \tilde{R}\rho_l(s) \equiv \frac{d}{5}\rho_l\left(\frac{s}{c}\right) + \frac{4d}{5}\rho_l\left(\frac{2s}{c}\right). \quad (4)$$

In the infinite generation limit of the renormalisation group (RG) equation, if $\rho^*(s)$ denotes the fixed point distribution such that $\rho^*(s) = \tilde{R}\rho^*(s)$, then assuming $\rho^*(s) \sim s^{-\gamma}\tilde{\rho}(s)$, one gets $(d/5)c^\gamma + (4d/5)(c/2)^\gamma = 1$. Here $\tilde{\rho}(s)$ represents an arbitrary modular function, which also includes a logarithmic correction for large s . This agrees with the above mentioned normalisation condition $cd = 5/3$ for the choice $\gamma = 1$. This result for the overlap distribution

$$\rho^*(s) \equiv \rho(s) \sim s^{-\gamma}; \quad \gamma = 1, \quad (5)$$

is the general result [13] for all cases that we have investigated and solved by the functional rescaling technique (with the $\log s$ correction for large s ,

renormalising the total integrated distribution). They include overlaps of different non-random Cantor sets, as well as higher dimensional fractals (for slides along various directions) like the carpet whose first generation is shown in Fig. 4. Also, by combining weighted probabilities for two such nonrandom fractals, one can generate recursion relations like (4) for the overlap distribution function for random fractals, which is the realistic case. One again gets the same result (5), except that the modular part $\tilde{\rho}(s)$ is periodic or quasi-periodic for general non-random fractals, and is normally constant for the random fractals. For all these cases, one gets the general result (5) for all the fractal surfaces. An obvious exception is where either (or both) of the surfaces is compact (Euclidean); there the distribution retains the original form, Fig. 3(a), in the successive generations and consequently gives $\gamma = 0$. It may be mentioned here that, in the context of flow through fractured media (underground mineral oil recovery), considerable investigations have already been made [14] on the scaling behaviour in the aperture of the channels between two rough fractured solid surfaces, even as one surface slides over the other. We investigate here a different aspect of the problem, namely the contact area distribution of such surfaces, as one slides over the other.

It may now be argued that the elastic energy ϵ stored between the two microscopically rough surfaces will be approximately proportional to the contact area s between the two surfaces. This is because during the sticking period, the solid-solid friction arises due to the elastic forces caused by elastic strains of the contact asperities of the surfaces [10]. Of course, the densities of slips of size s are not evenly distributed. As the tectonic plate moves with a constant velocity, we can assume that for a slip of contact area s the typical distance to be moved, and hence the time taken, will be of the order of s^δ , with $\delta = 1/D$ where D is the fractal dimensionality of the surfaces. This suggests that for a finite-time-average statistics, the number density $n(\epsilon)$ of quakes releasing energy ϵ will be given by

$$n(\epsilon) \sim \epsilon^{-(\gamma+\delta)}, \quad (6)$$

where $\gamma = 1$, and $\delta = 1/D$. This in turn implies that the number density $N(\epsilon)$ of quakes releasing energy greater than ϵ is given by

$$N(\epsilon) = \int_\epsilon^\infty n(\epsilon') d\epsilon' \sim \epsilon^{-\alpha}; \quad \alpha = \gamma + \delta - 1 = \delta, \quad (7)$$

with $\delta = 1/D$. This gives us the Guttenberg-Richter power law (3) with $\alpha = 1/D$. As the contact-surface fractal dimension D (given by the roughness exponent ζ discussed earlier) is generally less than two, our theory predicts the value of α to be greater than 0.5. This may be compared with its observed value ranging between 0.7 and 1.0.

3. Discussions

As emphasized already, we agree with the physicists' identification of the Guttenberg-Richter law (3) as an extremely significant one in geophysics. Like the previous attempts [4-6], we also develop here a model to capture this important feature in its resulting statistics. Judging from the comparisons of the exponent values α in (3) and (7), the model succeeds at least as well as the earlier ones. More importantly, our model incorporates both the geologically observed facts: fractal nature of the contact surfaces of the crust and of the tectonic plate [7-9], and the stick-slip motion between them [1,2]. However, the origin of the power law in the quake statistics here is the self-similarity of the fractal surfaces, and not any self-organisation directly in their dynamics. In fact, the extreme non-linearity in the nature of the crack propagation [3,8] is responsible for the fractal nature of the rough crack surfaces of the crust and the tectonic plate. This in turn leads here to the Guttenberg-Richter like power law in the earthquake statistics.

Acknowledgements: BKC is grateful to the Exchange Programme between the Indian National Science Academy and the Royal Society for supporting his visit to the Physics Department, Oxford University, Oxford, where this work was done. We are grateful to G. Ananthakrishna, A. Hansen, H. J. Herrmann, D. Fisher, S. S. Manna S. Roux for J. P. Vilotte for useful information, comments and criticisms.

References:

- [1] B. Guttenberg and C. F. Richter, *Seismicity of the Earth and Associated Phenomena*, Princeton Univ. Press, Princeton, N.J. (1954).
- [2] B. V. Kostrov and S. Das, *Principles of Earthquake Source Mechanics*, Cambridge Univ. Press, Cambridge (1988); C. H. Scholz, *The Mechanics of Earthquake and Faulting*, Cambridge Univ. Press, Cambridge (1990).

- [3] B. K. Chakrabarti and L. G. Benguigui, *Statistical Physics of Fracture and Breakdown in Disordered Solids*, Oxford Univ. Press, Oxford (1997).
- [4] R. Burridge and L. Knopoff, *Bull. Seis. Soc. Am.* **57** 341-371 (1967).
- [5] J. M. Carlson and J. S. Langer, *Phys. Rev. Lett.* **62** 2632-2635 (1989); J. M. Carlson, J. S. Langer and B. E. Shaw, *Rev. Mod. Phys.* **66** 657-670 (1994).
- [6] P. Bak, C. Tang and K. Wiesenfeld, *Phys. Rev. Lett.* **59** 381-384 (1987); P. Bak and C. Tang, *J. Geophys. Res.* **94** 15635-15637; Z. Olami, H. J. S. Feder and K. Christensen, *Phys. Rev. Lett.* **68** 1244-1247 (1992).
- [7] B. B. Mandelbrot, D. E. Passoja and A. J. Pullay, *Nature* **308** 721-722 (1984).
- [8] J. P. Bouchaud, E. Bouchaud, G. Lapasset and J. Planes, *Phys. Rev. Lett.* **71** 2240-2243 (1993); Marder, M. & Feinberg, J. *Phys. Today*, September, 24-29 (1996); Chakrabarti and B. K. Chakrabarti, *Physica A* (this Proc. Vol., 1999).
- [9] Y. Y. Kagan, *Geophys. J. Royal Astrophys. Soc. Canada* **71** 659 (1982); B. Barriere, and D. L. Turcotte, *Geophys. Res. Lett.* **18** 2011-2014 (1991); M. Sahimi, M. Robertson, *Physica A* **191** 57-68 (1992).
- [10] C. Caroli and Ph. Nozieres, *Eur. Phys. J. B* **4** 233-246 (1998).
- [11] B. B. Mandelbrot, *Fractal Geometry of Nature*, Freeman Press, New York (1982).
- [12] J. A. Ashraff, J. -M. Luck and R. B. Stinchcombe, *Phys. Rev. B* **41** 4314-4329 (1990) – Appendix B considers the Cantor Set convolution.
- [13] Such results can be checked by dealing explicitly with the large l behaviour of an appropriately rescaled version of the actual $\rho_l(s)$ resulting from $\tilde{R}^l \rho_0(s)$.
- [14] F. Plouraboué, P. Kurowski, J. P. Hulin, S. Roux, and J. Schmittbuhl, *Phys. Rev. E* **51** 1675-1685 (1995), and references therein.

Figure Captions:

Fig. 1. (a) Schematic representations of a portion of the rough surfaces of the earth's crust and the supporting (moving) tectonic plate. (b) The one

dimensional projection of the surfaces form Cantor sets of varying contacts or overlaps as one surface slides over the other.

Fig. 2. (a) Two cantor sets (in their first generation) along the axes r and $r - r'$. (b) This gives the overlap $s_1(r)$ along the diagonal. (c) The corresponding density $\rho_1(s)$ of the overlap s at this generation.

Fig. 3. The overlap densities $\rho(s)$ at various generations of the Cantor sets: at the zeroth (a), first (b), second (c) and at the infinite (or fixed point) (d) generations.

Fig. 4. Slides of two fractal carpets. The shaded regions indicate the material content portions of the surfaces at the second generation of an iterative construction of a fractal surface which is a Cantor set in each of the orthogonal directions. The overlap of the two carpets, for an arbitrary slide of one over the other, can be calculated by generalisation of the technique used to obtain (4).

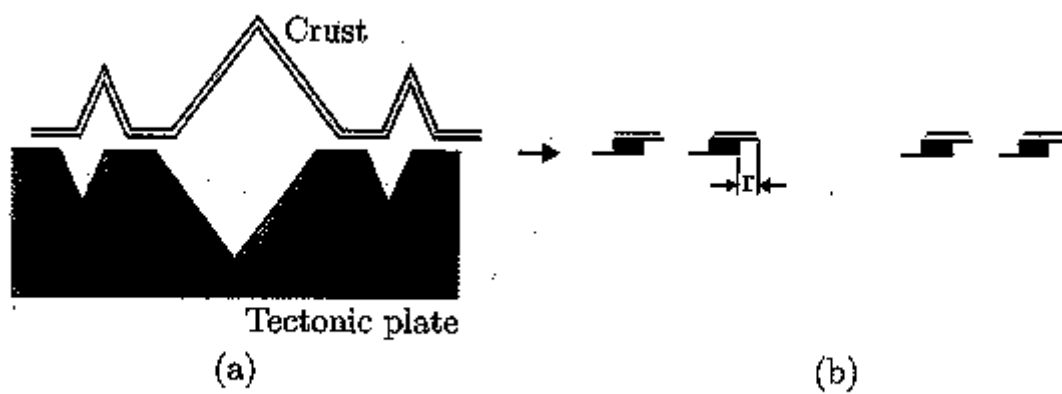


Fig. 1

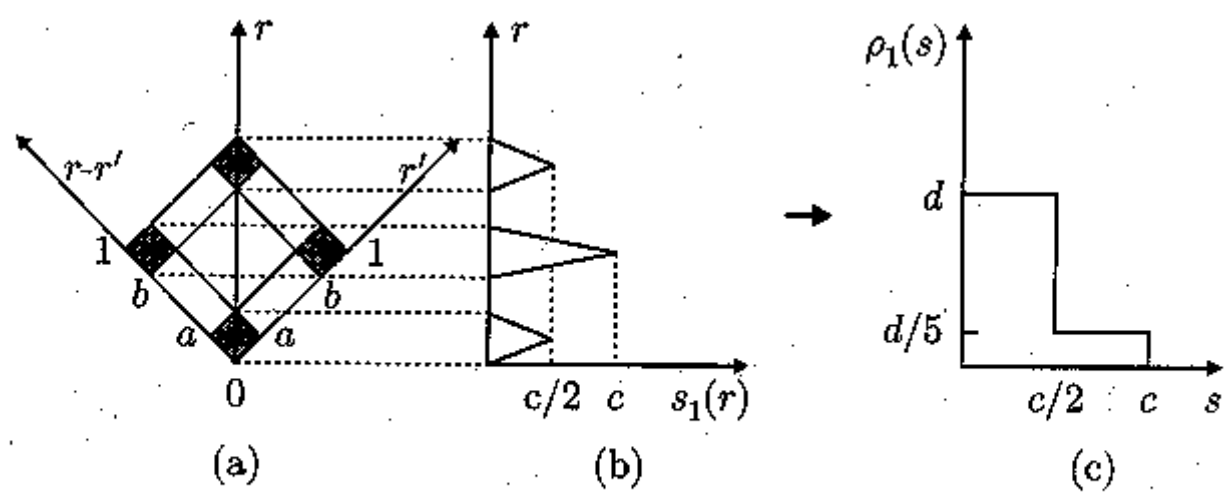


Fig. 2

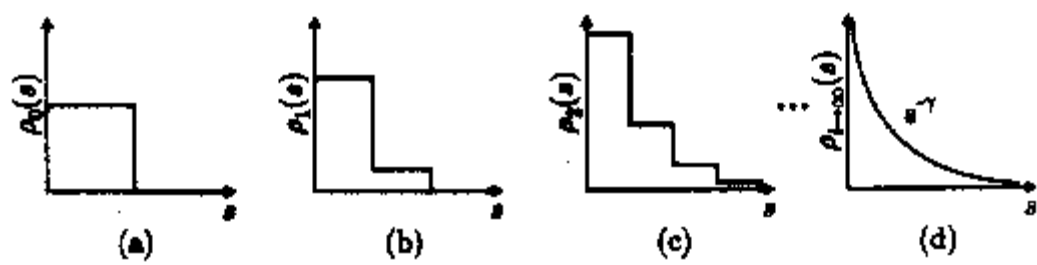


Fig. 3

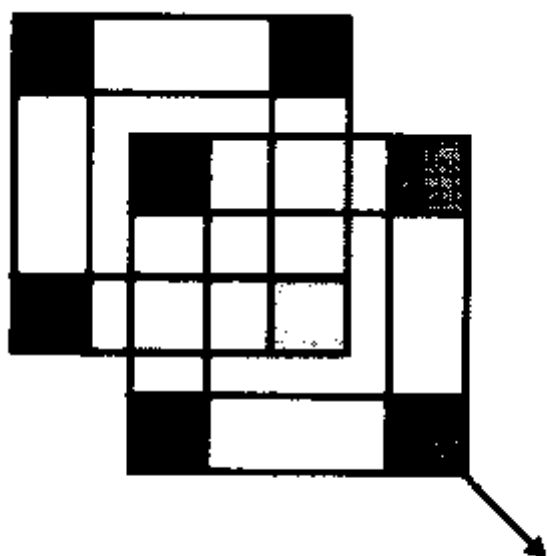


Fig. 4